processes

MDPI

Article

Molecular Geochemical Characteristics and Geological Significance of the Well B6 Crude Oil of the Tarim Basin

Taohua He [1,2,3,4,5,*], Yuanzhen Zhou [4], Jiayi He [4] and Jin Xu [1,2,3]

[1] State Key Laboratory of Shale Oil and Gas Enrichment Mechanisms and Effective Development, Beijing 100083, China; xujin.syky@sinopec.com
[2] SINOPEC Key Laboratory of Petroleum Accumulation Mechanisms, Wuxi 214126, China
[3] Research Institute of Exploration and Development, Sinopec Jianghan Oilfield Company, Wuhan 430223, China
[4] Hubei Key Laboratory of Petroleum Geochemistry and Environment, Yangtze University, Wuhan 430100, China; 2025710676@yangtzeu.edu.cn (Y.Z.); 2024720583@yangtzeu.edu.cn (J.H.)
[5] State Key Laboratory of Deep Oil and Gas, China University of Petroleum, Qingdao 266580, China
* Correspondence: hetaohua@yangtzeu.edu.cn

Abstract

Multiple biomarker datasets and compound-specific sulfur isotopic compositions ($\delta^{34}S$) of dibenzothiophenes (DBTs) were analyzed for crude oil from Well B6 on the Maigaiti Slope, Tarim Basin. The very low concentrations of DBTs (124.9 μg/g oil), diamondoids (92.7 μg/g oil), and thiadiamondoids (0.20 μg/g oil), together with the absence of 25-norhopane, indicate that the B6 oil has not undergone significant secondary alteration, including thermochemical sulfate reduction (TSR), extensive thermal cracking, or biodegradation. No clear evidence of oil mixing was observed either. Aliphatic and aromatic biomarker distributions suggest that the parent source rocks contain type I–II_1 kerogen, with dominant algal and bacterial organic inputs deposited under low-salinity, weakly reducing conditions, broadly comparable to those of the Upper Ordovician Lianglitag Formation source rocks (UOLS). Oil–source correlation using compound-specific $\delta^{34}S$ values of DBTs indicates that B6 oil is derived from UOLS (or similar undiscovered source rocks), not from Cambrian source rocks. This is consistent with biomarker evidence. As the first identified Ordovician-derived oil showing relatively light DBT $\delta^{34}S$ values (average ~6.41‰), close to those of Ordovician kerogen (average ~5.62‰), and with minimal secondary overprinting, B6 oil has strong potential to serve as a UOLS end-member oil. This will likely open new exploration opportunities for deep hydrocarbon from previously untapped strata in the southwestern Tarim Basin.

Keywords: thiadiamondoids; secondary alterations; oil-source correlation; deep hydrocarbon; Tarim basin

Academic Editor: Qingbang Meng

Received: 29 March 2026
Revised: 28 April 2026
Accepted: 12 May 2026
Published: 17 May 2026

1. Introduction

The Tarim Basin is one of the most hydrocarbon-rich cratonic basins in China. It covers ~46 × 10^4 km^2 and is surrounded by the ancient Kunlun Ocean, the ancient South Tianshan Ocean, and the Ku-Man troughs. Hydrocarbon occurrences include gas, condensate, light oil, waxy oil, heavy oil, and solid bitumen [1–3]. These accumulations have been widely linked to two major source intervals. One is the Cambrian–Lower Ordovician source rocks, represented by the Yuertusi Formation ($\epsilon_1 y$) mudstone/shale. The other is the Middle–Upper Ordovician source rocks, represented by the Lianglitag Formation ($O_3 l$) argillaceous

limestone [1,4–8]. However, the dominant contributor remains debated. A key reason is that unequivocal end-member oils have not been established [1]. Most discovered oils are either mixed or strongly altered. For example, oil from Well YM2 (3598–6050 m) was once regarded as an Ordovician end-member based on stable aromatic biomarker distributions. However, the presence of abundant aryl isoprenoids (AIs) indicates a green sulfur bacteria signal related to photic-zone anoxia typical of $\epsilon_1 y$ deposition [1,7,9], implying mixed sourcing.

In recent years, compound-specific sulfur isotopes ($\delta^{34}S$) have emerged as an effective tool for oil–source correlation. This is because sulfur isotopic fractionation during kerogen-to-oil conversion is generally limited in unaltered to weakly altered systems [6,10,11]. Secondary processes such as the thermochemical sulfate reduction (TSR), microbial sulfate reduction (MSR), and biodegradation may significantly broaden $\delta^{34}S$ ranges. This has been reported for Smackover oils and TSR-altered Tarim oils [6,10,12]. Previously reported Tarim oils mostly show relatively heavy $\delta^{34}S$ values (>+10‰). These values are consistent with Cambrian sources and inconsistent with Ordovician kerogens [6,10], suggesting that a robust Ordovician isotopic end member has not yet been identified.

To address this issue, this study integrates molecular biomarkers and compound-specific $\delta^{34}S$ of DBTs for oil from the Well B6 (5507–5588 m), evaluates secondary alteration and mixing effects, and constrains source affinity. The results indicate minimal secondary overprinting and strong geochemical affinity with $O_3 l$ source rocks, suggesting that B6 oil may represent a candidate Ordovician end-member oil.

2. Geological Background

The Maigaiti Slope is an important secondary tectonic unit within the southwestern Tarim Depression of the southwestern Tarim Basin (Figure 1). It trends NW–SE and forms a regional slope that dips gently toward the southwest. The Maigaiti Slope is bounded by the Keping Uplift to the northwest, the Bachu Uplift to the north, and the Tanguzibas Depression to the southeast. Tectonically, it represents a complex structural zone shaped by successive and superimposed deformation phases, including the Caledonian, Hercynian, Indosinian–Yanshanian, and Himalayan orogenic events. These multistage tectonic movements collectively produced the present-day macro-scale petroleum distribution pattern, characterized broadly as "oil in the west and gas in the east" across this slope. Owing to its favorable structural position and hydrocarbon potential, the Maigaiti Slope is regarded as a strategic exploration target in the southwestern Tarim region. The Bashituo oilfield, already discovered within this structural belt, demonstrates the area's significant and commercially relevant hydrocarbon endowment [13].

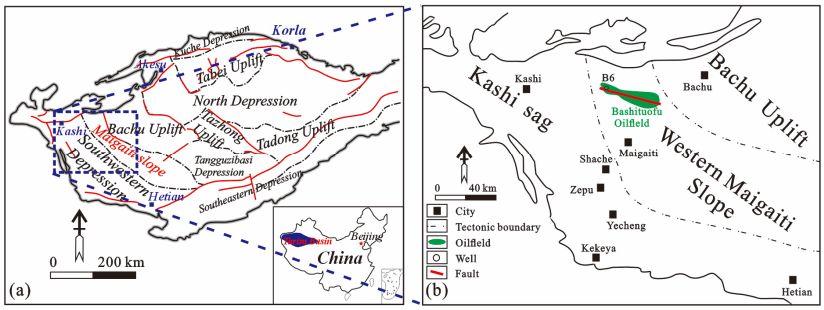

Figure 1. Simplified tectonic map of Tarim Basin in China (**a**) and the location of the well B6 (**b**).

Multiple sets of potential source rocks have been identified on the Maigaiti Slope and its surrounding areas, spanning the Cambrian, Ordovician, and Carboniferous systems. Among these, the Lower Cambrian Yuertusi Formation ($\epsilon_1 y$) black shale and siliceous mudstone is widely recognized as the highest-quality source rock in the region. This forma-

tion is characterized by exceptionally high total organic carbon (TOC) content, commonly exceeding 5%, with predominantly type I–II kerogen. At present, $\epsilon_1 y$ source rocks are in a high-to-over-mature stage (Ro generally > 2.0%), indicating a prolonged and sustained hydrocarbon-generation history, making them the dominant regional source interval [1,4,5]. The Middle–Upper Ordovician also contains marine source rocks with significant generative potential. In particular, the $O_3 l$ argillaceous limestone, developed in platform-margin to slope facies settings within the eastern Maigaiti Slope and the adjacent Tanguzibas Depression, satisfies the critical conditions for effective source rock development. Organic matter in $O_3 l$ source rocks is predominantly type I–II kerogen, with Ro values reaching ~1.3% in some areas, placing these rocks at the peak oil generation stage [7,14]. Carboniferous source rocks, by contrast, were deposited mainly in lagoonal and swamp environments; their organic matter is of relatively lower quality and predominantly gas-prone, thus playing a secondary role in the regional petroleum system.

The structural framework of the Maigaiti Slope has been strongly influenced by the migration of paleo-uplifts, particularly the Hetian paleo-uplift. During the Caledonian and Hercynian periods, the crest of the paleo-uplift served as the preferred locus of early hydrocarbon migration and entrapment. The petroleum migration and accumulation system is dominated by fault networks and unconformity surfaces. Specifically, strike-slip and thrust faults active during the Late Hercynian and Himalayan stages served as key vertical conduits connecting deep source rock intervals to shallower reservoir units [13,14]. Although no $O_3 l$ source rocks have been reported in the study area, potential equivalents may exist in the adjacent Tanguzibas Depression. Hydrocarbons generated from such deep source rocks could have migrated laterally over long distances via major regional unconformities (e.g., the Caledonian and Hercynian unconformities) and accumulated on the Maigaiti Slope [13,14].

The Bashituo oilfield is located in the Qunkeqiake structural belt in the northwestern part of the Maigaiti Slope. The Well B6 is one of the key exploratory wells in this oilfield, and its crude oil is primarily produced from the Devonian Donghetang Formation sandstone. Conventional interpretation has long attributed the oils in this area predominantly to the highly mature to overmature Cambrian source rocks [15]. However, significant differences exist between the molecular geochemical signatures of B6 oil and those expected from Cambrian-sourced systems, necessitating a rigorous and systematic oil–source investigation. This study, therefore, focuses on the crude oil from Well B6 as an object to identify its precise source affinity through multiple lines of geochemical evidence.

3. Sample and Methods

The crude oil sample analyzed in this study was collected from Well B6 (5507–5588 m) in the Bashituo oilfield on the Maigaiti Slope, southwestern Tarim Basin. For comparative evaluation of geochemical parameters and oil–source correlation, a suite of reference samples was also incorporated. These include the once-proposed Cambrian end-member oil from Well TD2 (4630–4670 m), the once-proposed Ordovician end-member oil from Well YM2 (3598–6050 m) [1], and six representative Cambrian and Ordovician source rock samples from the Tarim Basin previously documented in our earlier works [2,7,9]. For each sample, biomarker ratios and compound-specific sulfur isotope values were measured three times, and the average value was taken as the final result. Systematic molecular geochemical and compound-specific sulfur isotope analyses were carried out in previous works [7,8,10]. The mean standard deviation of $\delta^{34}S$ values for thiadamantanes in the sulfidic fraction was typically better than 2‰ (1σ) with an instrument reproducibility of ±0.8‰ [10]. And the accuracy of the analyses of biomarker ratios was estimated to be better than 2%.

3.1. Separation of Crude Oil Group Compositions

Oil group fractions were separated using silver ion exchange liquid chromatography. A Pasteur pipette was first packed with approximately 300 mg of $AgNO_3$-impregnated silica gel (200 mesh silica gel soaked in 10% $AgNO_3$ solution, then activated at 105 °C for 3 h), followed by a layer of activated silica gel (40 μm, 60 Å; activated at 225 °C for 16 h). Approximately 50 mg of crude oil was weighed and spiked with d_{16}-adamantane and dioctyl sulfide as internal standards for quantitative analysis of diamondoid and sulfur-containing compounds, respectively. Asphaltene was first precipitated from the crude oil by the addition of excess n-hexane. The remaining maltene fraction was loaded onto the prepared column and eluted sequentially with n-hexane, dichloromethane, and acetone to obtain saturated hydrocarbon, aromatic hydrocarbon, and sulfur-containing compound fractions, respectively.

3.2. Gas Chromatography–Mass Spectrometry (GC-MS)

The saturated, aromatic, and sulfur-containing fractions were analyzed using an Agilent 6890N/5975B gas chromatography–mass spectrometry instrument (Agilent Technologies, Santa Clara, CA, USA). For saturated hydrocarbon analysis, an HP-5MS fused silica capillary column (30 m × 0.25 mm i.d. × 0.25 μm film thickness, Agilent Technologies, USA) was used. The carrier gas was He at a constant flow of 1.04 mL/min. The injector temperature was set at 300 °C. The GC oven temperature program was as follows: an initial hold at 50 °C for 2 min, a ramp from 50 to 100 °C at 20 °C/min, then a ramp from 100 to 310 °C at 3 °C/min, with a final isothermal hold at 310 °C for 15.5 min. The mass spectrometer was operated in electron ionization (EI) mode at 70 eV. Data acquisition used both selective ion monitoring (SIM) and full-scan detection (FSD) modes. C_{29} androstane was used as a quantitative internal standard. For aromatic hydrocarbon analysis, a DB-5MS column (60 m × 0.25 mm i.d. × 0.25 μm film thickness) was employed. The He flow rate was held constant at 0.80 mL/min, and the injector temperature was 300 °C. The GC oven temperature was programmed from 80 °C (3 min hold), then to 230 °C at 3 °C/min, then to 300 °C at 2 °C/min, with a 17 min isothermal hold. The EI conditions were 70 eV, with an emission current of 300 μA and a multiplier voltage of 1000 V. Both SIM and FSD modes were applied. d_{10}-naphthalene and dibenzothiophene served as internal standards for quantification. For analysis of sulfur-containing compounds, an HP-1 capillary column (60 m × 0.32 mm i.d. × 0.25 μm film thickness) was used with He at 1.10 mL/min. The oven temperature was held at 70 °C for 5 min, ramped to 290 °C at 3 °C/min, and then held isothermally for 20 min. EI energy was 70 eV, and the ion source temperature was set at 250 °C.

4. Results

4.1. Aliphatic Hydrocarbons

The total ion chromatogram (TIC) of aliphatic hydrocarbons from B6 oil shows a clear dominance of low-carbon-number n-alkanes with chain lengths predominantly below n-C_{19}, with the distribution maximum at n-C_{15} (Figure 2a,d,e,g; Table 1). No appreciable unresolved complex mixture (UCM) hump is observed in the baseline, indicating that the oil has not suffered significant biodegradation. This n-alkane distribution pattern is consistent with a major contribution from lower aquatic organisms, such as algae and bacteria [16]. The carbon preference index (CPI) and odd-to-even predominance (OEP) are both approximately 1.0, indicating that the oil was generated from thermally mature source rocks at or near the main oil generation stage with no pronounced odd-over-even or even-over-odd carbon number preference.

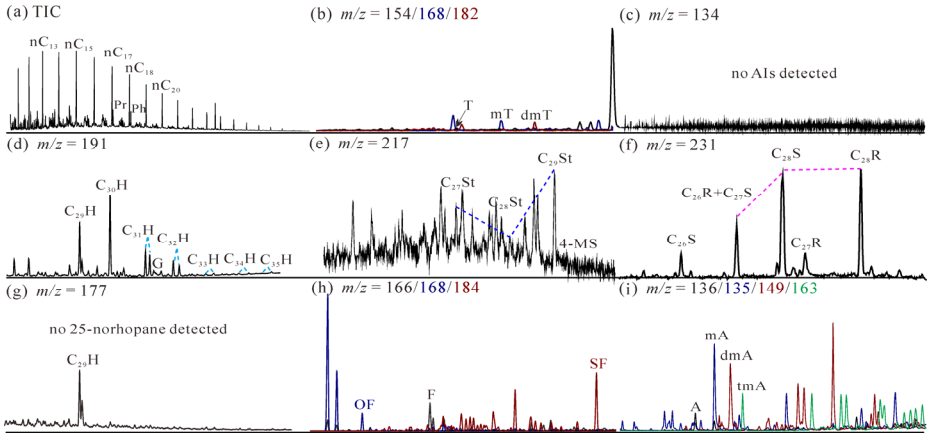

Figure 2. Partial mass chromatograms of n-alkane (**a**), terpanes (**d**,**g**), steranes (**e**), aromatic hydrocarbon (**c**,**f**,**h**), adamantane (**i**), and 2-thioadamantanes (**b**) of the crude oil from well B6 (TIC: total ion chromatogram; compound identification symbols are explained in Table 1).

Table 1. Abbreviations for mass fragmentograms compound in saturate fractions (1), aromatic fractions (2), adamantanes (3), thioadamantanes (4), and biomarker ratios (5).

Abbreviations	Meanings	Abbreviations	Meanings
(1) Saturate fractions			
$C_{29}H$	17α(H), 21β(H)-30-Norhopane	$C_{32}H$	C_{32} 17α, 21β(H)-homohopane
G	Gammacerane	$C_{33}H$	C_{33} 17α, 21β(H)-homohopane
$C_{30}H$	$\alpha\beta$ C_{30} hopane	$C_{34}H$	C_{34} 17α, 21β(H)-homohopane
$C_{31}H$	C_{31} 17α, 21β(H)-homohopane	$C_{35}H$	C_{35} 17α, 21β(H)-homohopane
Pr	Pristane	Ph	Phytane
C_{27} St	C_{27} 20R-5α, 14α(H), 17α(H)-steranes	C_{29} St	C_{29} 20R-5α, 14α(H), 17α(H)-steranes
C_{28} St	C_{28} 20R-5α, 14α(H), 17α(H)-steranes	4-MS	C_{30} 4-methylsteranes
(2) Aromatic fractions			
$C_{26}S$	C_{26} 20R-triaromatic sterane	$C_{28}S$	C_{28} 20S-triaromatic sterane
$C_{27}R$	C_{27} 20R-triaromatic sterane	$C_{28}R$	C_{28} 20R-triaromatic sterane
$C_{26}R + C_{27}S$	C_{26} 20R + C_{27} 20S-triaromatic steranes	AIs	aryl isoprenoids
SF	Dibenzothiophene (DBT)	OF	Dibenzofuran
F	Fluorene	DBTs	Dibenzothiophenes
TDS	Triaromatic dinosterane	MeTAS	3-methyl-24-ethyl-triaromatic sterane
P	Phenanthrene	MP	Methylphenanthrene
(3) Adamantanes			
A	Adamantane	mA	Methyladamantane
dmA	Dimethyladamantane	tmA	Trimethyladamantane
(4) Thioadamantanes			
T	2-thioadamantanes	mT	1-methyl-2-thioadamantanes
dmT	1,3-dimethyl-2-thioadamantanes		
(5) Main biomarker ratios			
4-MSI	4-methylsteranes/C_{29} sterane	TDSI	$\sum$TDS/($\sum$TDS + $\sum$METS)
C_{28}/C_{29} St	C_{28}/C_{29} 20R-5α, 14α(H), 17α(H)-steranes	G/C_{31}HR	gammacerane/$\alpha\beta C_{31}$ homohopane 22R
C_{27}/C_{29} St	C_{27}/C_{29} 20R-5α, 14α(H), 17α(H)-steranes	Pr/Ph	pristane/phytane
C_{28}/C_{26-28} TAS	$C_{28}/(C_{26} + C_{27} + C_{28})$ triaromatic steranes	SF/OF	Dibenzothiophene/Dibenzofuran
S/H	$\sum$steranes/$\sum$hopanes		
R*cb*	0.40 + 0.6 × (TNR-2)	R*c*	0.40 + 0.6 × (MPI-1)
TNR-2	Trimethylnaphthalene (TMN) ratio 2 = (2,3,6- + 1,3,7-TMN)/(1,4,6- + 1,3,5- + 1,3,6-TMN)		
MPI-1	MP index 1 = 1.5 × (3-MP + 2-MP)/(P + 1-MP + 9-MP)		

The abundance of pristane (Pr) is slightly higher than that of phytane (Ph), yielding a Pr/Ph ratio of 1.06, falling within the weakly reducing range [16]. Notably, both Pr and Ph are present in relatively low abundances compared with their adjacent n-alkanes, as reflected by Pr/n-C_{17} and Ph/n-C_{18} ratios of 0.53 and 0.68, respectively, suggesting limited input from diagenetically reworked chlorophyll-derived phytol under prolonged anoxic conditions.

Examination of m/z 191 and m/z 177 mass chromatograms reveals the absence of 25-norhopane, a diagnostic marker for severe biodegradation, and near-absence of gammacerane (G), with a gammacerane index (G/C_{31}HR; ratio of gammacerane to C_{31} 17α, 21β(H)-homohopane 22R) of only 0.11. The m/z 217 mass chromatogram shows no detectable 4-methylsteranes (4-MS), and a clear predominance of C_{29} regular steranes (20R-5α, 14α(H), 17α(H)-sterane; C_{29} St) among the C_{27}–C_{29} sterane series. The ratios of C_{27}/C_{29} St, C_{28}/C_{29} St, and 4-MSI (4-MS/C_{29} St) are 0.38, 0.52, and 0, respectively (Table 2; Figure 3). The total sterane-to-hopane ratio (S/H) is 0.69, which is broadly comparable to that of Ordovician source rocks. Sterane isomerization parameters, $S/(S + R)$ C_{29} sterane [20S/(20S + 20R) 14α(H), 17α(H)-ethylcholestane] and $\beta/(\beta + \alpha)$ C_{29} sterane [14β(H), 17β(H)/(14α(H), 17α(H) + 14β(H), 17β(H)) 20R-ethylcholestane], are 0.47 and 0.55, respectively. These values are below the established equilibrium ranges of 0.52–0.55 and 0.67–0.71 [17,18], confirming a mature but sub-equilibrium thermal state.

Table 2. Selected geochemical parameters calculated from source rocks and crude oils in the Tarim Basin.

ID	C1 [a]	C2	C3	Y1 [b]	Y2	Y3	L1 [c]	L2	L3
Well/Outcrop	B6	TD2	YM2	LT1	Outcrop	LT3	TZ30	TZ12	LN46
Depth/m	5570–5588	4630–4670	3598–6050	8654.39	6.58	8518.31	4918.56	4817.27	6164.81
Strata	D	$\in$	O	$\in_1 y$	$\in_1 y$	$\in_1 y$	$O_3 l$	$O_3 l$	$O_3 l$
Oil/source rock	Crude oil	Crude oil	Crude oil	Source rock	Source rock	Source rock	Source rock	Source rock	Source rock
C_{27}/C_{29} St	0.38	1.04	0.68	1.44	1.22	1.32	0.73	0.42	0.67
C_{28}/C_{29} St	0.52	0.78	0.56	0.88	0.75	0.56	0.51	0.48	0.52
4-MSI	~0	0.38	~0	0.47	0.47	0.36	0.04	~0	0.01
C_{28}/C_{26-28} TAS	0.67	0.38	0.72	0.41	0.38	0.32	0.64	0.74	0.59
(C_{26}R + C_{27}S)/C_{28}S	0.46	1.47	0.43	1.36	1.54	1.85	0.56	0.61	0.44
TDSI	0.24	0.77	0.19	0.75	0.85	0.66	0.16	0.34	0.27
S/H	0.69	0.97	0.58	1.24	1.34	1.16	0.59	0.72	0.53
25-norhopane/C_{29}H	~0	~0	0.09	~0	~0	~0	~0	~0	~0
Pr/n-C_{17}	0.53	0.26	0.44	0.31	0.37	0.44	0.58	0.61	0.64
Ph/n-C_{18}	0.68	0.39	0.52	0.38	0.48	0.54	0.62	0.65	0.71
Pr/Ph	1.06	0.72	0.89	0.81	0.54	0.55	1.07	0.97	1.15
AIs	−	+	+	+	+	+	−	−	−
C_{27}R/C_{28}R	0.36	0.75	0.31	0.65	0.85	1.25	0.31	0.46	0.57
C_{26}S/C_{28}S	0.17	0.46	0.15	0.96	0.75	0.74	0.15	0.24	0.16
G/C_{31}HR	0.11	0.88	0.31	0.92	1.19	0.83	0.14	0.25	0.33
SF/OF	3.16	36.24	8.14	34.38	116.91	27.2	2.1	0.88	3.87
R*cb*	0.94	1.13	0.89	1.04	0.97	1.07	0.91	0.87	0.91
R*c*	0.91	1.17	0.88	1.07	1.04	1.08	0.93	0.76	0.82

Note: ID, Identification symbol; [a], crude oil 1; [b], source rock 1 from the Lower Cambrian Yuertusi Formation ($\in_1 y$); [c], source rock 1from the $O_3 l$; −, absent; +, abundant; Biomarkers and their ratios calculation could be seen in Table 1.

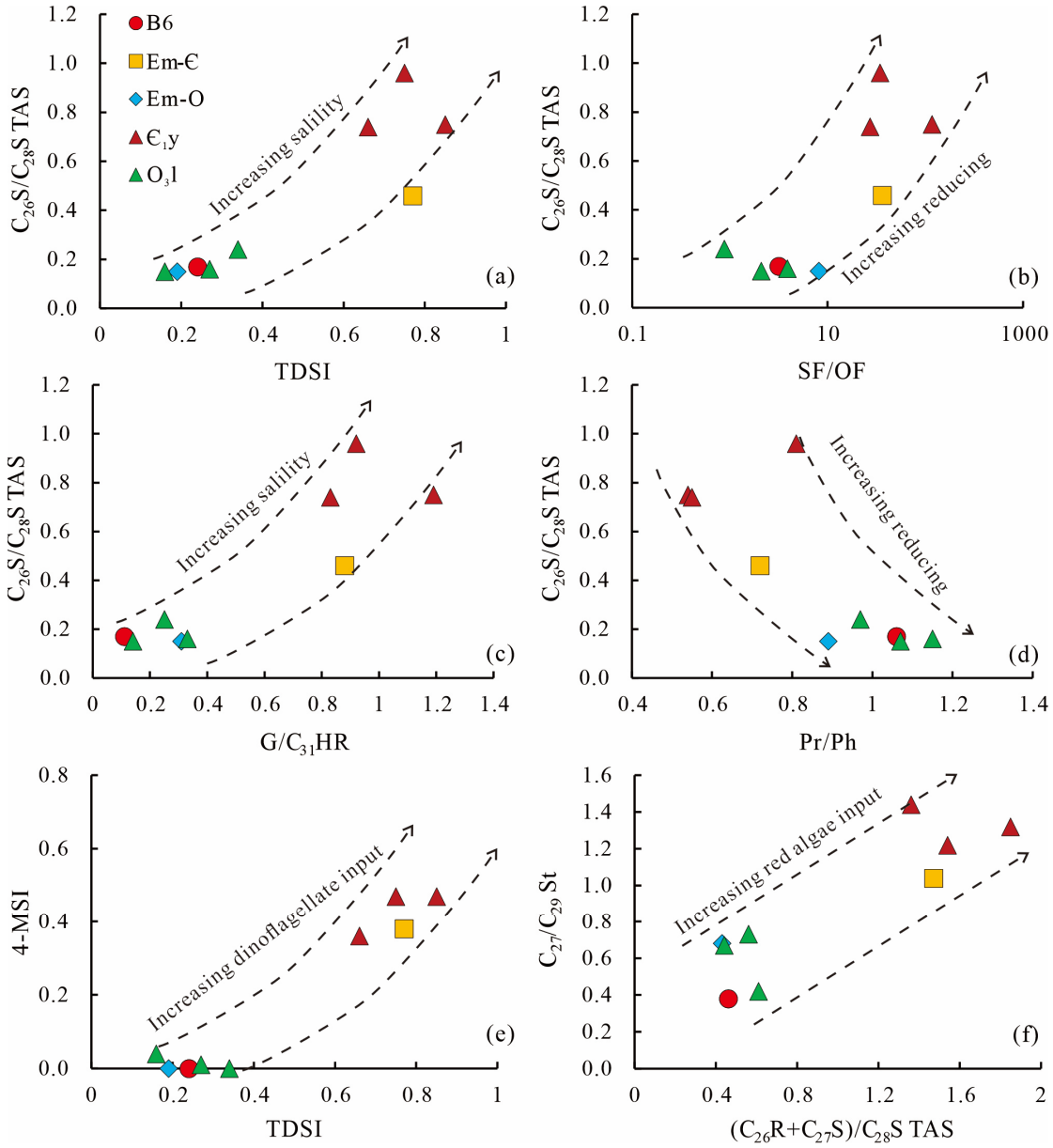

Figure 3. Crossplots among biomarker parameters for the oils and source rocks in the Tarim Basin ((**a**) crossplots between $C_{26}S/C_{28}S$ TAS and TDSI; (**b**) crossplots between $C_{26}S/C_{28}S$ TAS and SF/OF; (**c**) crossplots between $C_{26}S/C_{28}S$ TAS and $G/C_{31}HR$; (**d**) crossplots between $C_{26}S/C_{28}S$ TAS and Pr/Ph; (**e**) crossplots between 4-MSI and TDSI; (**f**) crossplots between C_{27}/C_{29} St and $(C_{26}R + C_{27}S)/C_{28}S$ TAS; biomarker parameters are explained in Table 1).

4.2. Aromatic Hydrocarbons

Aromatic hydrocarbons investigated in this study include aryl isoprenoids (AIs), triaromatic steranes (TASs), triaromatic dinosteranes (TDSs), and the trifluorene series consisting of dibenzothiophene (DBT), dibenzofuran (OF), and fluorene (F) (Figure 2c,f,h). No identifiable AIs were detected in B6 oil in either the *m*/*z* 133 or *m*/*z* 134 mass chromatograms in SIM or FSD detection mode. For comparison, a series of AIs were clearly identified in reference oils TD2, YM2, ZS1C, and TZ83 and in $Є_1y$ source rock extracts analyzed using the same pre-treatment and analytical procedure (Figures 2c and 4). The complete absence of AIs in B6 oil is an important negative indicator, as discussed in Section 5.1.

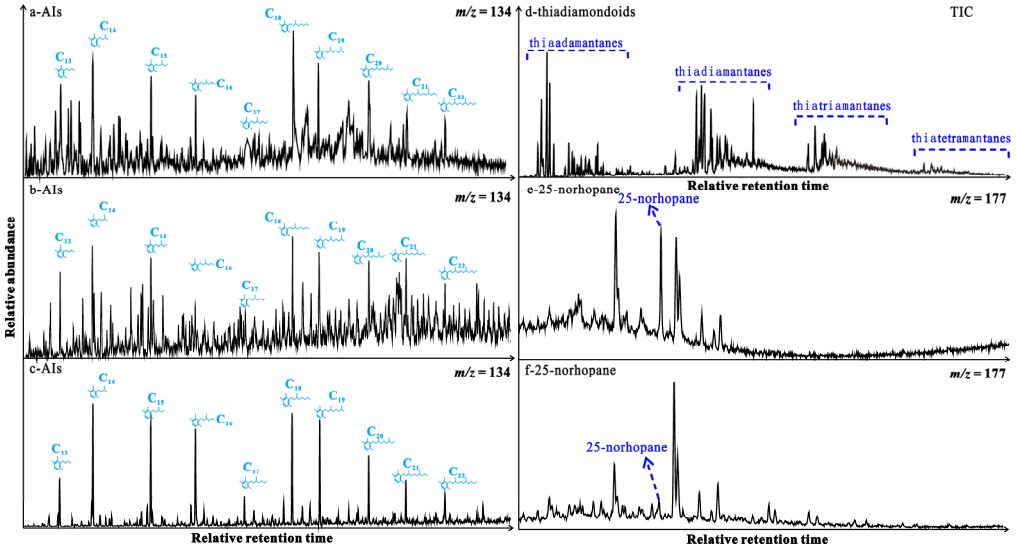

Figure 4. Mass chromatograms of AIs, thiadiamondoids, and 25-norhopane in crude oils ((**a**,**d**) crude oil from the well ZS1C (6861–6944 m, Є); (**b**,**e**) crude oil from the well TZ83 (5433–5441 m, O_3l); (**c**,**f**) a reference crude oil from the well YM2 (3597.68–6050 m, O)).

In the *m*/*z* 231 chromatogram, TAS distributions in B6 oil include C_{26}S, C_{27}R, C_{26}R + C_{27}S, C_{28}S, and C_{28}R tria + The calculated ratios of $C_{28}/C_{26–28}$ TAS, (C_{26}R + C_{27}S)/C_{28}S, C_{27}R/C_{28}R, and C_{26}S/C_{28}S are 0.67, 0.46, 0.36, and 0.17, respectively (Table 2). Triaromatic dinosteranes (TDSs) are present in notably lower abundances than 3-methyl-24-ethyl-triaromatic steranes (MeTASs), with a TDS index [TDSI = ΣTDSs/(ΣTDSs + ΣMeTASs)] of 0.24, similar to that of YM2 oil but considerably lower than that of TD2 oil (Table 2). In the trifluorene series, the relative abundance follows the order DBT > F > OF, with a DBT/OF (SF/OF) ratio of 3.16. The total DBT concentration quantified in B6 oil is 124.9 μg/g oil. Aromatic hydrocarbon maturity parameters were also calculated: calculated vitrinite reflectance values R*c* and R*cb*, based on methylphenanthrene and trimethylnaphthalene distributions, respectively (calculation procedure detailed in Table 1), are 0.81% and 0.91%, placing B6 oil in the late main-stage oil window.

Compound-specific δ^{34}S values were successfully measured for multiple alkyl-DBT compounds in B6 oil. The values range from 3.80‰ to 9.98‰, with an arithmetic mean of 6.41‰. Among the identified compounds, 2,4-/2,6-/3,6-dimethyl-DBTs yield the heaviest δ^{34}S values, reaching up to ~9.98‰ [19]. Despite this intra-compound variation, the overall average δ^{34}S of B6 oil is substantially lighter than that of most crude oils previously analyzed from the Tazhong and Tabei Uplifts. For comparison, the Well ZS1C oil (6902.5 m, Tazhong Uplift) shows δ^{34}S values of 33.57–40.79‰ (avg. 37.09‰), and the Well YM2 oil (4823.8 m, Tabei Uplift) shows 14.39–22.32‰ (avg. 17.72‰) [6,10,20]. The distinctly lighter sulfur isotopic composition of B6 oil compared with both reference oils suggests a fundamentally different source rock input for the B6 system.

4.3. Adamantines and Thioadamantanes

Compared with oils from the Tazhong Uplift reported previously (e.g., Well ZS1C oil with diamondoid concentrations of ~155,000 μg/g oil and thiadiamondoid concentrations of ~8578 μg/g oil) [6,10,21], B6 oil contains notably low concentrations of both adamantane-type diamondoids and their sulfur analogs. Recognizable thiadiamondoids in the *m*/*z* 154/168/182 mass chromatograms include 2-thioadamantane, methyl-2-thioadamantanes, and dimethyl-2-thioadamantanes (Figure 2b), with a quantified total thiadiamondoid concentration of only 0.20 μg/g oil. Recognizable diamondoids in the *m*/*z* 136/135/149/163 mass chromatograms include adamantane, methyl-adamantanes,

dimethyl-adamantanes, and trimethyl-adamantanes, together with diamantane, methyl-diamantanes, and dimethyl-diamantanes in the m/z 188/187/201 mass chromatograms (Figure 2i). Total diamondoid (adamantanes + diamantanes) concentration is 92.67 μg/g oil (Table 2).

5. Discussions

5.1. Evaluation of Secondary Alteration and Oil Mixing

Secondary alteration and multistage mixing represent two of the most significant processes complicating geochemical interpretation in Tarim Basin oils [1,22]. Before discussing depositional environment and oil–source correlation, it is necessary to systematically evaluate whether B6 oil has experienced any of the following major secondary processes: TSR alteration, thermal cracking, biodegradation, or oil mixing.

(1) Assessment of TSR Alteration

Thermochemical sulfate reduction (TSR) is a high-temperature inorganic sulfate reduction process driven by hydrocarbons reacting with sulfate minerals (typically anhydrite or gypsum), which commonly generates H_2S, CO_2, elemental sulfur, and sulfur-bearing organic compounds, including DBTs and thiadiamondoids [23,24]. Due to their highly stable cage-shaped carbon skeleton, diamondoids are extremely resistant to thermal and chemical alteration and thus serve as reliable benchmarks for quantifying TSR-driven sulfur incorporation and oil cracking extents [25,26]. When TSR operates, a sulfur atom replaces a carbon vertex in the diamondoid cage, forming thiadiamondoids, which are stable and accumulate in oil as diagnostic TSR indicators [23]. Accordingly, simultaneous enrichment of DBTs, diamondoids, and thiadiamondoids is a hallmark of TSR-altered oils.

A well-characterized reference dataset from Smackover-derived oils of the US Gulf Coast clearly distinguishes TSR-unaltered oils (DBTs: 45–431 μg/g oil, avg. 173 μg/g; diamondoids: 22–357 μg/g oil, avg. 150 μg/g; thiadiamondoids: 0–120 μg/g oil, avg. 42 μg/g) from TSR-altered oils (DBTs: 691–6313 μg/g oil, avg. 1927 μg/g; diamondoids: 512–8668 μg/g oil, avg. 3943 μg/g; thiadiamondoids: 180–1745 μg/g oil, avg. 649 μg/g) [24]. B6 oil contains only 124.9 μg/g DBTs, 92.7 μg/g diamondoids, and 0.2 μg/g thiadiamondoids (Figure 5). These concentrations fall well within the TSR-unaltered range and are orders of magnitude lower than those of severely TSR-altered Tarim oils such as Well ZS1C (diamondoids ~155,000 μg/g oil; thiadiamondoids ~4400 μg/g oil; DBTs ~70,000 μg/g oil) [10]. These data collectively demonstrate that B6 oil has not undergone any significant TSR alteration.

(2) Assessment of Thermal Alteration

The thermal maturity of B6 oil was evaluated using a combination of saturated and aromatic biomarker parameters. C_{29} sterane isomerization ratios, $S/(S + R)$ = 0.47 and $\beta/(\beta + \alpha)$ = 0.55, are below their established equilibrium endpoints, arguing against generation from highly to overmature source rocks. It is important to note that these sterane-based parameters may lose discriminatory power at high maturities once equilibrium is reached, making aromatic maturity proxies more reliable in such contexts [27–29]. Calculated vitrinite reflectance values from methylphenanthrene (Rc = 0.81%) and trimethylnaphthalene (Rcb = 0.91%) independently confirm that B6 oil falls within the late main-stage oil window, which is consistent with the expected thermal maturity of O_3l source rocks and comparable to that of YM2 oil. These values are substantially lower than those expected from overmature $Є_1y$-sourced systems (Figure 6). Furthermore, the low total diamondoid concentration (92.67 μg/g oil) is inconsistent with substantial thermal cracking, which typically generates and enriches diamondoids as n-alkane chains are progressively cracked at high temperatures [26]. Taken together, these observations confirm that B6 oil has not been subjected to significant thermal alteration or secondary thermal cracking.

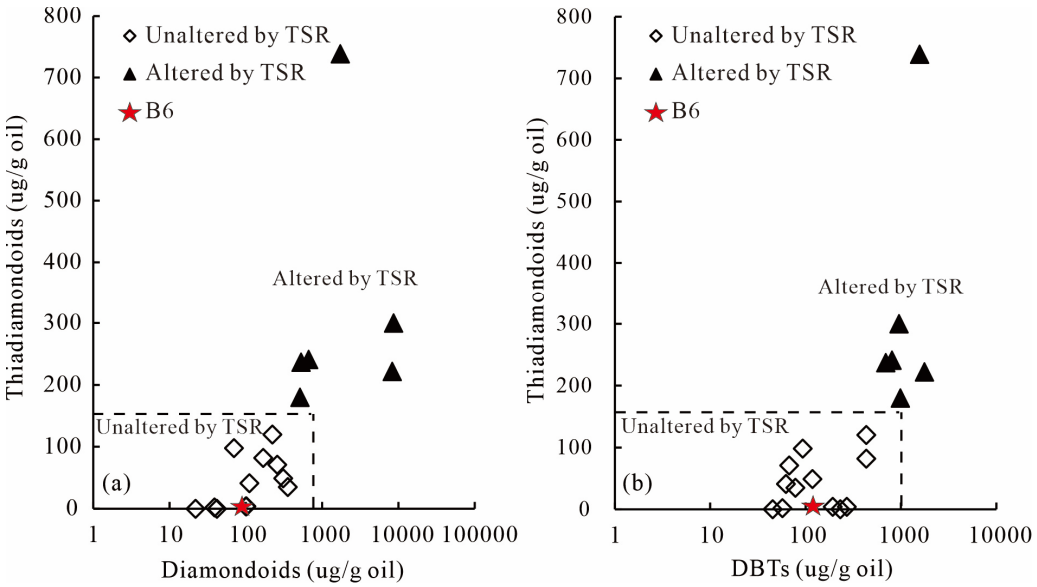

Figure 5. Crossplots among thiadiamondoids, diamondoids, and DBTs (note: DBTs, dibenzothiophenes; altered-TSR and unaltered-TSR data are from the northern Gulf of Mexico reported by [24]). (**a**) crossplots between thiadiamondoids and diamondoids; (**b**) crossplots between thiadiamondoids and DBTs.

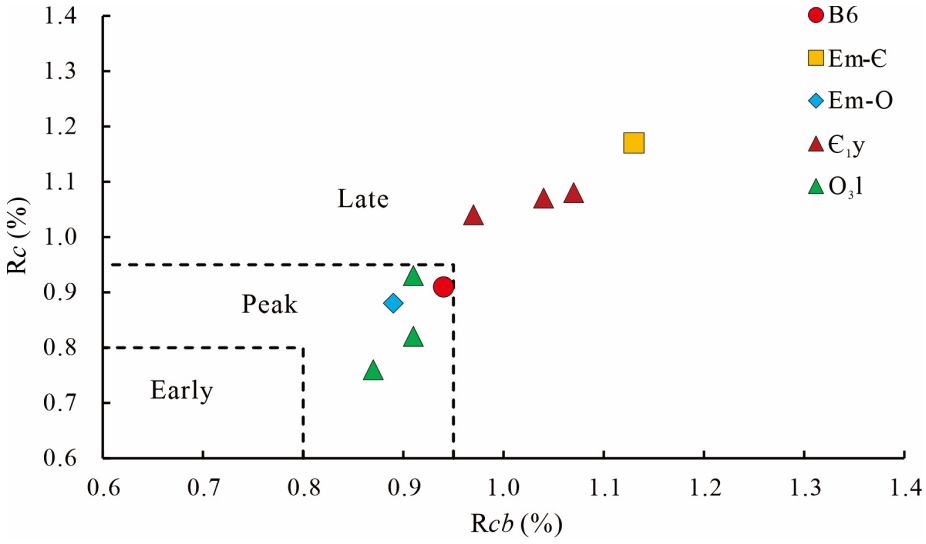

Figure 6. Thermal maturity cross-plot of calculated vitrinite reflectance R*c* (MPI-1; [27] and R*cb* (TNR-2; [28]), respectively.

(3) Assessment of Biodegradation Alteration

Biodegradation, carried out primarily by subsurface microbial communities including eubacteria, fungi, and possibly archaea [4,16], progressively removes compounds in order of decreasing bioavailability. In its early stages (PM level < 3 on the Peters–Moldowan scale; [30]), characteristic features include the loss of n-alkanes, the development of a UCM hump in the TIC, and the appearance of 25-norhopanes generated via microbial demethylation of hopanes [16]. In B6 oil, the TIC shows a well-resolved and continuous distribution of n-alkanes from n-C_{11} to n-C_{29} with no discernible UCM, and 25-norhopanes are entirely absent (25-norhopane/C_{29}H ~ 0). These features unequivocally indicate that B6 oil has not undergone significant biodegradation, even at the lowest detectable levels on the PM scale.

(4) Assessment of Mixing Events

Oil mixing between Cambrian-sourced and Ordovician-sourced end members is widespread in the Tarim Basin and significantly complicates source attribution [1,20]. Key biomarker parameters for distinguishing these two source types include AIs, TAS-related parameters, TDSI, and SF/OF ratios. $\in_1$y-sourced oils typically contain abundant AIs reflecting green sulfur bacteria input under photic-zone euxinic conditions, alongside higher TDSI and $C_{26}S/C_{28}S$ ratios, and lower C_{28}/C_{26-28} TAS ratios [2,31,32]. Ordovician O_3l-sourced oils show the opposite patterns: absent or trace AIs, lower TDSI, and higher C_{28}/C_{26-28} TAS ratios. Crucially, AIs exhibit exceptional resistance to thermal alteration, TSR alteration, and biodegradation, as demonstrated by their preservation in both severely TSR-altered oil from Well ZS1C and severely biodegraded oil from Well TZ83 (Figure 4). Therefore, the complete absence of AIs in B6 oil is a highly reliable negative indicator for Cambrian source contribution. Consistent with this, TAS distributions, TDSI, $C_{26}S/C_{28}S$ ratio, and SF/OF ratio all align closely with O_3l source rock signatures rather than $\in_1$y patterns (Figures 2 and 3; Table 2). No evidence of mixed Cambrian–Ordovician biomarker signals is observed.

In summary, B6 oil has experienced no significant TSR alteration, thermal cracking, biodegradation, or mixing. Its primary geochemical signatures are well preserved, making it suitable for reliable depositional environment reconstruction and oil–source correlation.

5.2. Depositional Environment of Parent Source Rocks

Having established the absence of significant secondary alteration in B6 oil, its aliphatic and aromatic biomarker distributions can be used to constrain the depositional environment of its parent source rocks.

The gammacerane index ($G/C_{31}HR$ = 0.11) and the $C_{26}S/C_{28}S$ ratio (0.17) are among the lowest values recorded across all analyzed samples in this study (Table 2). The $C_{26}S/C_{28}S$ ratio of 0.17 is well below the value of 0.21 established for confirmed freshwater depositional settings [33,34], suggesting that the parent source rocks were deposited under low-salinity to near-freshwater conditions. This is consistent with the known paleogeographic setting of O_3l argillaceous limestone, which was deposited in a shallow-water carbonate platform or platform-margin environment, characterized by relatively open marine circulation with limited evaporitic restriction [1]. The positive covariation between $G/C_{31}HR$ and $C_{26}S/C_{28}S$ observed across the studied sample suite (Figure 3) further confirms that both parameters track water column salinity stratification, with B6 oil occupying the low-salinity end of the spectrum.

Redox-sensitive parameters reinforce the above interpretation. The Pr/Ph ratio of B6 oil is 1.06, falling in the range of 1.0–3.0, indicative of weakly reducing (suboxic) conditions [35,36]. The DBT/OF (SF/OF) ratio of 3.16 is the lowest among the analyzed oils and source rock samples (Figure 3b), consistent with a less sulfur-enriched, weakly reducing depositional setting rather than strongly euxinic conditions that would be expected for the $\in_1$y deep-water restricted basin environment [37]. The negative correlation between Pr/Ph and $C_{26}S/C_{28}S$ ratio (Figure 3d) and positive correlation between DBT/OF and $C_{26}S/C_{28}S$ ratio (Figure 3b) across all samples indicates that elevated salinity tends to promote anoxic conditions, whereas B6 oil distinctly clusters at the low-salinity, weakly reducing end. These results are further supported by the ternary diagram of DBT, OF, and F (Figure 7), which shows B6 oil plotting in the weakly reducing zone consistent with O_3l-type source rocks.

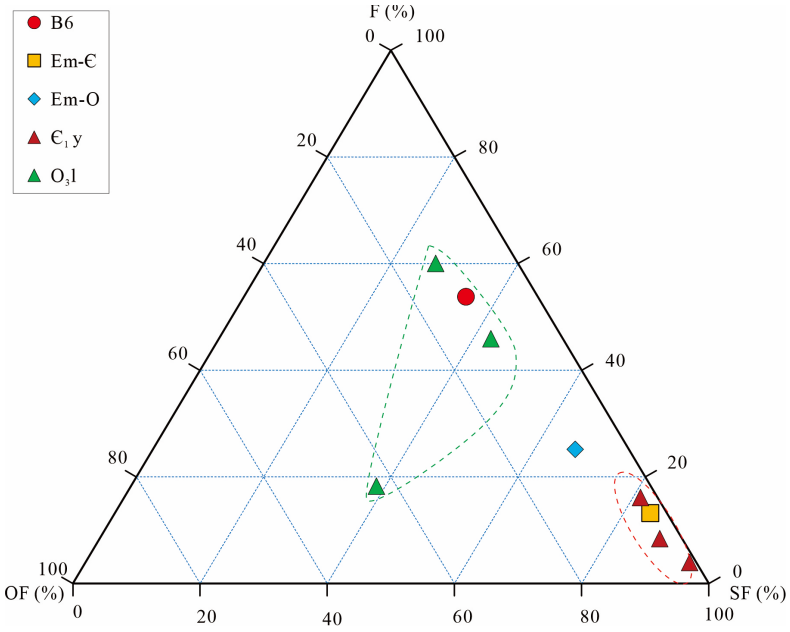

Figure 7. A ternary plot of SF, OF, and F of source rocks and crude oils in the Tarim Basin.

5.3. Organic Matter Sources of the Parent Rocks

The cross-plot of Pr/n-C_{17} versus Ph/n-C_{18} ratios for B6 oil plots within the field of type I–II_1 kerogen derived from Lower Paleozoic marine source rocks (Figure 8), indicating a dominant contribution from aquatic algae and/or bacteria in a marine depositional environment. This is consistent with the pre-Devonian geological record, during which higher land plants had not yet evolved, and organic matter was overwhelmingly derived from marine algae and prokaryotic bacteria [16].

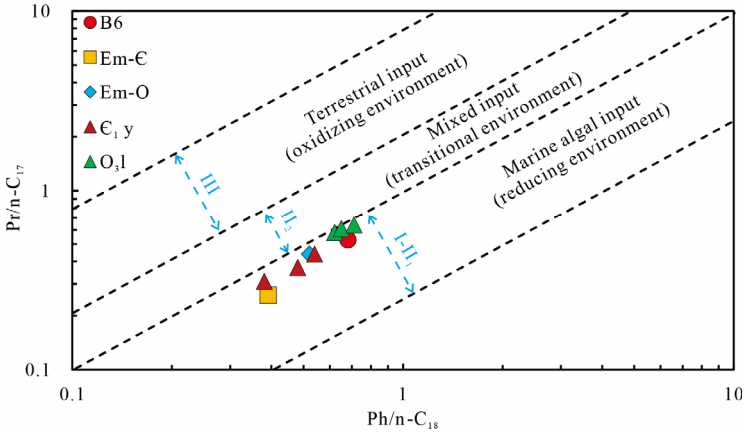

Figure 8. Crossplot of Pr/n-C_{17} versus Ph/n-C_{18} ratios of source rocks and crude oils in the Tarim Basin.

More specific attribution of organic sources is possible through biomarker ratios sensitive to distinct algal groups and dinoflagellates. In the pre-Devonian, C_{27} regular steranes are predominantly derived from red algae (Rhodophyta), whereas C_{29} regular steranes have stronger contributions from green algae (Chlorophyta). Their respective final aromatic products are C_{26} TAS and C_{28} TAS [2,16,38]. The 4-methylsteranes (4-MS) originate predominantly from dinoflagellates, and their aromatization product is TDS [39,40]. In B6 oil, the relatively lower C_{27}/C_{29} St ratio (0.38) and ($C_{26}R + C_{27}S)/C_{28}S$ ratio (0.46), combined with the higher $C_{28}/C_{26–28}$ TAS ratio (0.67) and near-zero TDSI (0.24), collectively suggest a dominant green algal contribution with minor red algal and

dinoflagellate inputs. This is consistent with a shallow-water, low-salinity carbonate platform setting where green algae thrived, and red algae and dinoflagellates were less productive. Positive correlations among C_{27}/C_{29} St, $(C_{26}R + C_{27}S)/C_{28}S$, and $C_{26}S/C_{28}S$ ratios across the study samples (Figure 3a,e,f) further demonstrate that salinity exerts a first-order control on algal community composition: higher salinity preferentially supports red algae and dinoflagellate blooms, whereas green algae dominate under lower-salinity conditions. These results are depicted in the ternary diagram of C_{27} St, C_{28} St, and C_{29} St (Figure 9), where B6 oil plots in the C_{29}-dominant field, consistent with green algae-dominated organic matter input. The overall S/H ratio of 0.69 is broadly consistent with the mixed algal–bacterial input implied by type I–II_1 kerogen characterization.

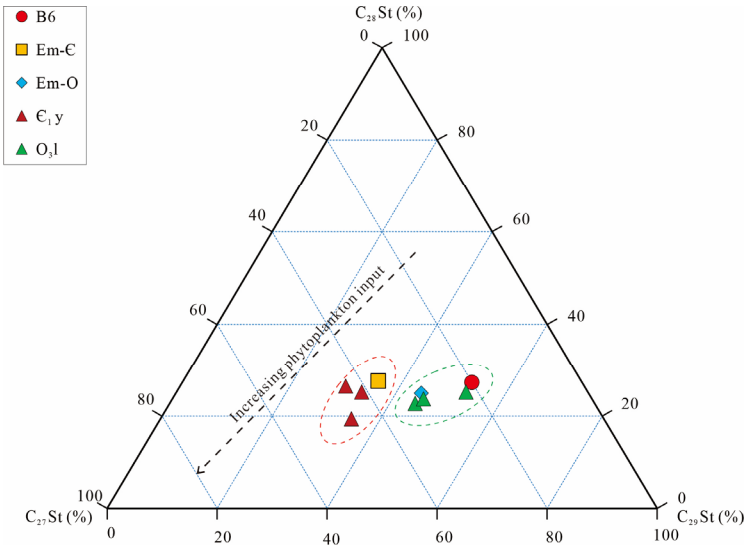

Figure 9. A ternary plot of C_{27} St, C_{28} St, and C_{29} St of source rocks and crude oils in the Tarim Basin.

5.4. Oil-Source Correlation Based on Compound-Specific $\delta^{34}S$

For compound-specific $\delta^{34}S$ to be reliably applied to oil–source correlation in the Tarim Basin, two principal criteria must be satisfied: (1) the analyzed oil must be free of significant secondary alteration, so that its $\delta^{34}S$ values still reflect those of the parent kerogen; and (2) the associated H_2S concentration should be below ~0.25%, confirming the absence of substantial thermochemical or bacterially mediated sulfate reduction [5,6,41,42]. As demonstrated in Section 5.1, B6 oil shows no clear evidence for TSR, thermal alteration, or biodegradation. Additionally, H_2S concentration is effectively 0% in B6 oil and in adjacent oils from Wells Qun2, Qun5 in the Bashituo oilfield [43]. Both criteria are therefore satisfied, providing a robust foundation for $\delta^{34}S$-based oil–source interpretation of B6 oil.

Previous compound-specific sulfur isotope studies have established clear $\delta^{34}S$ signatures for the two principal source rock intervals in the Tarim Basin [5,6]. Cambrian $Є_1y$ kerogens show relatively heavy $\delta^{34}S$ values ranging from 14.0‰ to 21.6‰ (avg. 19.1‰), reflecting deposition under strongly euxinic, sulfate-enriched bottom water conditions during the early Cambrian. By contrast, Middle–Upper Ordovician O_3l kerogens yield distinctly lighter $\delta^{34}S$ values of 2.9–7.8‰ (avg. 5.62‰), consistent with a less sulfidic, more oxic depositional setting. This ~13.5‰ difference in average kerogen $\delta^{34}S$ provides a well-defined isotopic contrast that, when primary oil signatures are preserved, can serve as an effective discriminator for oil–source correlation.

Previously analyzed crude oils from the Tazhong and Tabei Uplifts, with the exception of the severely TSR-altered ZS1C oil, exhibit compound-specific $\delta^{34}S$ values of DBTs ranging from 11.2‰ to 28.9‰ (avg. 20.3‰) in this study and from 10.2‰ to 22.5‰ (avg. 19.4‰) as reported in earlier work [5]. These values align closely with Cambrian kerogen $\delta^{34}S$,

confirming dominant Cambrian source contributions to oils in those uplifts. In sharp contrast, B6 oil yields DBT δ^{34}S values of 3.80–9.98‰ (avg. 6.41‰), which are markedly lighter than all Cambrian-correlated oils and fall directly within the range defined by Ordovician O_3l kerogens (Figure 10).

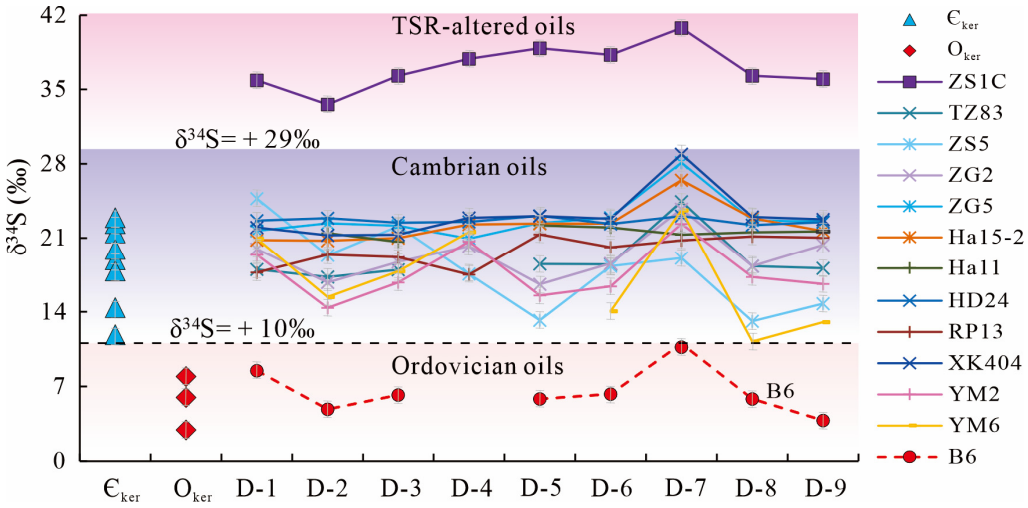

Figure 10. Oil-source correlation based on compound-specific δ^{34}S of alkyldibenzothiophenes and δ^{34}S of Cambrian-Ordovician kerogens in the Tarim Basin (ϵ_{ker}, kerogen of Cambrian source rocks; O_{ker}, kerogen of Ordovician source rocks; D-1, DBT; D-2, 4-MeDBT; D-3, 2 + 3-MeDBT; D-4, 1-MeDBT; D-5, 4-EtDBT; D-6, 4,6-DMeDBT; D-7, 2,4/2,6/3,6-DMeDBT; D-8, TMeDBT; D-9, TMeDBT; data of Cambrian-Ordovician kerogens are collected from these works [6,10,21]).

The geochemical significance of this isotopic match can be further quantified by considering the expected δ^{34}S offset between unaltered oil and its parent kerogen. Both case studies and pyrolysis simulation experiments of immature kerogen under dry and hydrous conditions have demonstrated that δ^{34}S values of oil derived from a given kerogen are generally within ±2‰ of the kerogen value, without significant systematic fractionation under thermally mild conditions [41,42,44]. In the case of B6 oil, the mean offset between B6 oil (avg. 6.41‰) and Ordovician kerogens (avg. 5.62‰) is only +0.81‰, well within the ±2‰ tolerance threshold. Conversely, the mean offset between B6 oil and Cambrian kerogens (avg. 19.1‰) is ~12.7‰, far exceeding this threshold and effectively ruling out any significant Cambrian contribution. Although minor contributions from Cambrian sources cannot be entirely excluded, the high sensitivity of sulfur isotopes to mixing—where even a small input from a heavy sulfur end-member would produce a detectable positive shift—supports the interpretation that the B6 oil is dominated by a single end-member. The absence of such a shift, together with the absence of TSR alteration, reinforces the candidate end-member status of the B6 oil. Thus, these quantitative comparisons strongly support the interpretation that B6 oil is exclusively or predominantly derived from Middle–Upper Ordovician source rocks.

This conclusion is independently and consistently supported by the extensive suite of aliphatic and aromatic biomarker evidence discussed in Sections 5.2 and 5.3. Specifically, the close alignment of B6 oil with O_3l source rock signatures on biomarker cross-plots (Figure 3), the ternary diagram of sterane compositions (Figure 9), the maturity cross-plot (Figure 6), and the fluorene ternary diagram (Figure 7) all converge on the same interpretation. Furthermore, the diagnostic absence of AIs in B6 oil, combined with low TDSI and low $C_{26}S/C_{28}S$ values, unequivocally rules out contributions from ϵ_1y source rocks. The consistency among multiple independent geochemical lines of evidence—isotopic,

aliphatic biomarker, and aromatic biomarker—substantially strengthens the reliability of the Ordovician source attribution for B6 oil (Figure 11).

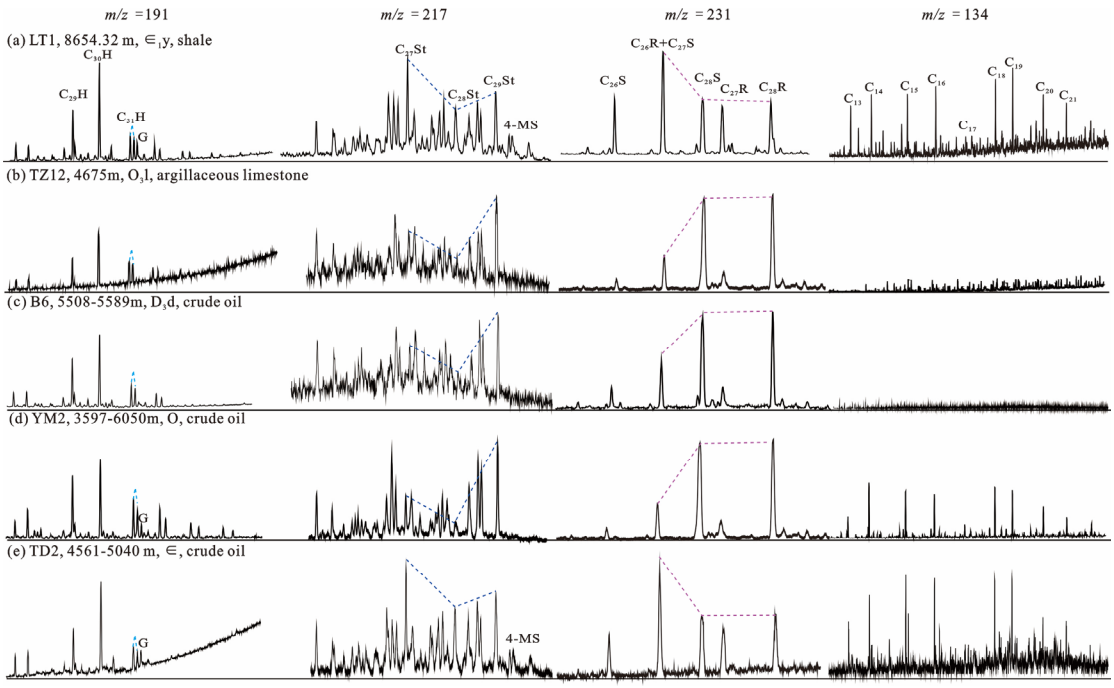

Figure 11. Oil-source correlation based on mass chromatograms of hopanes (m/z 191) and steranes (m/z 217) saturate fractions, as well as triaromatic steranes (m/z 231) and AIs (m/z 134) of source rocks and crude oils in the Tarim Basin (abbreviations are explained in Table 1).

It is worth noting that the observed slight enrichment of the heaviest $\delta^{34}S$ values in specific alkyl-DBT congeners (e.g., 2,4-/2,6-/3,6-dimethyl-DBTs reaching ~9.98‰) may reflect minor compound-specific isotopic heterogeneity inherited from the source kerogen rather than secondary alteration, since the overall range remains narrow (3.80–9.98‰) and consistent with primary source signatures rather than the wide range (often exceeding 20‰) typical of TSR-influenced systems [6,10,12]. This narrow isotopic spread further reinforces the faithful interpretation that B6 oil preserves its primary $\delta^{34}S$ signature.

5.5. Geological Significance

The persistent controversy over the relative contributions of Cambrian versus Ordovician source rocks to hydrocarbon accumulations in the Tarim Basin has, for several decades, defied resolution. The root cause, as summarized by Huang et al. [1], lies in the absence of reliably identified and geochemically unambiguous end-member oils. Without valid end members, quantitative mixing calculations and source proportioning remain fundamentally unconstrained.

The previously proposed Cambrian end-member oils include those from Wells TD2 (6430–6470 m), TZ62 (4053–4074 m), ZS1 (6426–6497 m), and ZS1C (6861–6944 m). The proposed Ordovician end-member oil from Well YM2 (3598–6050 m) was, for a time, the most widely cited candidate. However, systematic re-evaluation has revealed critical disqualifying factors for each: TD2 oil has experienced significant thermal alteration, TZ62 oil has been severely biodegraded, ZS1C oil has undergone extreme TSR alteration, and both ZS1 and YM2 oils contain mixed biomarker signatures indicative of combined Cambrian–Ordovician sourcing [1]. Specifically, the presence of abundant AIs in YM2 oil, a uniquely diagnostic Cambrian indicator, demonstrates that it cannot be treated as a pure Ordovician end member, regardless of its TAS-based similarities to Ordovician facies.

A geochemically valid end-member oil must fulfill two fundamental requirements: (1) it must not have undergone significant secondary alteration that could modify its primary geochemical fingerprint; and (2) it must not have experienced mixing with oils from other source rock types, preserving a single-source signal. As demonstrated systematically in Section 5.1, B6 oil satisfies both criteria. It shows no evidence of TSR alteration (extremely low diamondoids, thiadiamondoids, and DBTs), no evidence of significant thermal cracking (sub-equilibrium sterane isomerization, moderate R*c* and R*cb* values, and low diamondoid concentrations), and no evidence of biodegradation (intact n-alkane suite, no UCM, no 25-norhopanes). Moreover, the complete absence of AIs and the full suite of O_3l-consistent biomarker parameters unambiguously rule out mixing with Cambrian-sourced oil.

Among all known Tarim oils analyzed to date for compound-specific $\delta^{34}S$, B6 oil represents the first identified example of an Ordovician-derived crude oil with primary $\delta^{34}S$ values consistent with Ordovician kerogen. Its average DBT $\delta^{34}S$ of 6.41‰ is not only the lightest recorded among Tarim crude oils but also closely matches Ordovician O_3l kerogen $\delta^{34}S$ (avg. 5.62‰) within a margin smaller than the expected oil–kerogen isotopic fractionation. No other known Tarim oil satisfies this isotopic criterion while simultaneously meeting the secondary alteration and mixing exclusion criteria. This combination of characteristics is unique and constitutes a compelling case for designating B6 oil as a valid Ordovician end-member oil.

The practical significance of this designation extends beyond academic classification. In the Tarim Basin, many commercially important deep reservoirs—particularly in the Tazhong and Tabei Uplifts—contain complex mixed oils with contributions from both Cambrian and Ordovician source rocks in varying proportions [1,22]. Quantitative deconvolution of these mixed systems requires isotopically and geochemically defined end members at both extremes of the mixing array. While Cambrian end-member $\delta^{34}S$ values are relatively well constrained (avg. ~19–20‰), the Ordovician end-member $\delta^{34}S$ had previously been inferred only from kerogen data without a confirmed oil counterpart. B6 oil now provides this missing anchor point. By incorporating B6 oil's $\delta^{34}S$ (avg. ~6.41‰) and its associated biomarker fingerprint as the Ordovician end-member reference, future studies may more accurately and quantitatively resolve the proportional contributions of each source type to mixed deep oils across the basin. This has direct implications for resource assessment, exploration targeting, and understanding the long-term petroleum system evolution of the Tarim Basin.

Furthermore, the discovery of B6 oil as an Ordovician-sourced, minimally altered crude oil on the Maigaiti Slope suggests that pockets of Ordovician-dominated oil accumulations may exist in structurally favorable positions on the western and southwestern margins of the Tarim Basin, where Cambrian source rock contribution may be relatively limited compared with central uplift areas. This has important implications for future exploration strategy in the southwestern Tarim region, particularly in areas where Ordovician carbonate reservoirs and Devonian clastic reservoirs may be fed preferentially by the more proximal O_3l source system [19,45].

Finally, we have to admit that due to the limited number of core tests, the Ordovician strata in the study area have developed O_3l, but there have been no reports of source rocks in this formation. Therefore, the hydrocarbon source rocks referred to in this article may not rule out the possibility of undiscovered source rocks similar to O_3l, just as early predecessors predicted the existence of a set of undiscovered Cambrian source rocks developed in photic zone euxinia (PZE) environment, which enabled a prolific growth of photosynthetic green sulfur bacteria (Chlorobiaceae) in the Tarim Basin [4].

6. Conclusions

The following conclusions can be drawn from the systematic molecular geochemical and compound-specific sulfur isotope investigation of crude oil from Well B6 on the Maigaiti Slope, southwestern Tarim Basin:

(1) B6 oil has not undergone significant secondary alteration. It shows exceptionally low concentrations of DBTs (124.9 μg/g oil), diamondoids (92.67 μg/g oil), and thiadiamondoids (0.20 μg/g oil). It also completely lacks 25-norhopanes. The n-alkanes range from n-C_{11} to n-C_{29} with no unresolved complex mixture (UCM). Together, these features rule out meaningful TSR alteration, thermal cracking, and biodegradation. Aromatic maturity parameters (R*c* = 0.81%; R*cb* = 0.91%) independently confirm that this oil was generated within the late main-stage oil window. This is inconsistent with overmature Cambrian-sourced systems.

(2) Aliphatic and aromatic biomarker distributions of B6 oil indicate that its parent source rocks contained type I–II_1 kerogen with dominant inputs from marine algae (particularly green algae) and bacteria, deposited under low-salinity, weakly reducing conditions. These paleoenvironmental characteristics are broadly consistent with those of the O_3l argillaceous limestone, which was deposited in a shallow carbonate platform-to-platform-margin setting.

(3) B6 oil is the first crude oil from the Tarim Basin to exhibit compound-specific DBT δ^{34}S values (3.80–9.98‰; avg. ~6.41‰) falling unambiguously within the isotopic range of O_3l kerogens (2.9–7.8‰; avg. ~5.62‰). The mean oil–kerogen δ^{34}S offset is only +0.81‰, well within the ±2‰ expected fractionation limit for unaltered systems. In contrast, the large offset from Cambrian ϵ_1y kerogens (~12.7‰) effectively excludes any significant Cambrian contribution. This isotopic conclusion is independently corroborated by the full suite of aliphatic and aromatic biomarker evidence, including the diagnostic absence of AIs and the O_3l-consistent TAS, TDSI, and fluorene series distributions.

(4) B6 oil is proposed as a candidate Ordovician end-member oil for the Tarim Basin. Its compound-specific ^{34}S and biomarker fingerprints provide the first well-constrained Ordovician isotopic anchor point for quantitative deconvolution of complex mixed oils in the Tazhong and Tabei Uplifts. It may ultimately help resolve the long-standing and commercially significant oil–source controversy in the Tarim Basin.

Author Contributions: T.H.: Conceptualization, Writing—original draft, Funding Acquisition. Y.Z.: Data Curation, Writing—review and editing. J.H.: Software, Methodology. J.X.: Investigation. All authors have read and agreed to the published version of the manuscript.

Funding: This research was funded by the open fund of SINOPEC Key Laboratory of Petroleum Accumulation Mechanisms (NO. 33550007-22-ZC0613-0040), Sinopec Technology Research and Development Project (NO. KLP23016), and the National Natural Science Foundation of China (NO. 42272160).

Data Availability Statement: The original contributions presented in this study are included in the article. Further inquiries can be directed to the corresponding author.

Acknowledgments: Gratitude is expressed for the financial support provided, and special thanks are given to Qilin Xiao from the Key Laboratory of Oil and Gas Resources and Exploration Technology, Yangtze University, Wuhan, for his help with 2-thiadiamidoid analysis. We also acknowledge the precious advice of the editors and reviewers.

Conflicts of Interest: Authors Taohua He and Jin Xu were employed by the Sinopec Jianghan Oilfield Company. The remaining authors declare that the research was conducted in the absence of any commercial or financial relationships that could be construed as a potential conflict of interest. The company had no role in the design of the study; in the collection, analyses, or interpretation of data; in the writing of the manuscript, or in the decision to publish the results.

References

1. Huang, H.; Zhang, S.; Su, J. Palaeozoic oil-source correlation in the Tarim Basin, NW China: A review. *Org. Geochem.* **2016**, *94*, 32–46. [CrossRef]
2. He, T.; Lu, S.; Li, W.; Wang, W.; Sun, D.; Pan, W.; Zhang, B. Geochemical characteristics and effectiveness of thick, black shales in southwestern depression, Tarim Basin. *J. Petrol. Sci. Eng.* **2020**, *185*, 106607. [CrossRef]
3. He, T.; He, J.; Xu, J.; Wang, H.; Zhou, Y.; Xue, K.; Xu, Y. Integration of PINN with Conventional Well Logging for Few-Shot TOC Prediction in Ultradeep Source Rocks. *ACS Omega* **2026**, *11*, 4581–4596. [CrossRef]
4. Sun, Y.; Xu, S.; Lu, H.; Cuai, P. Source facies of the Paleozoic petroleum systems in the Tabei uplift, Tarim Basin, NW China: Implications from aryl isoprenoids in crude oils. *Org. Geochem.* **2003**, *34*, 629–634. [CrossRef]
5. Cai, C.; Li, K.; Ma, A.; Zhang, C.; Xu, Z.; Worden, R.H.; Wu, G.; Zhang, B.; Chen, L. Distinguishing Cambrian from Upper Ordovician source rocks: Evidence from sulfur isotopes and biomarkers in the Tarim Basin. *Org. Geochem.* **2009**, *40*, 755–768. [CrossRef]
6. Cai, C.; Zhang, C.; Worden, R.H.; Wang, T.; Li, H.; Jiang, L.; Huang, S.; Zhang, B. Application of sulfur and carbon isotopes to oil–source rock correlation: A case study from the Tazhong area, Tarim Basin, China. *Org. Geochem.* **2015**, *83*, 140–152. [CrossRef]
7. He, T.; Li, W.; Lu, S.; Pan, W.; Ying, J.; Zhu, P.; Yang, E.; Wang, X.; Zhang, B.; Sun, D. Mechanism and geological significance of anomalous negative $\delta^{13}C_{kerogen}$ in the Lower Cambrian, NW Tarim Basin, China. *J. Petrol. Sci. Eng.* **2022**, *208*, 109384. [CrossRef]
8. Zeng, Q.; He, T.; Zhao, Y.; Zhang, K.; Wen, Z.; Xu, Y.; He, J.; Tian, W.; Lu, S.; Cheng, W.; et al. Geochemical characteristic of different-lithofacies source rocks and its implications for ultradeep hydrocarbon exploration in the lower cambrian Yuertus formation, Tarim basin. *Sci. Rep.* **2025**, *15*, 24071. [CrossRef] [PubMed]
9. He, T.; Lu, S.; Li, W.; Sun, D.; Pan, W.; Zhang, B.; Tan, Z.; Ying, J. Paleoweathering, hydrothermal activity and organic matter enrichment during the formation of earliest Cambrian black strata in the northwest Tarim Basin, China. *J. Petrol. Sci. Eng.* **2020**, *189*, 106987. [CrossRef]
10. Cai, C.; Amrani, A.; Worden, R.H.; Xiao, Q.; Wang, T.; Gvirtzman, Z.; Li, H.; Said-Ahmad, W.; Jia, L. Sulfur isotopic compositions of individual organosulfur compounds and their genetic links in the lower paleozoic petroleum pools of the Tarim Basin, NW China. *Geochim. Cosmochim. Acta* **2016**, *182*, 88–108. [CrossRef]
11. Greenwood, P.F.; Mohammed, L.; Grice, K.; McCulloch, M.; Schwark, L. The application of compound-specific sulfur isotopes to the oil-source rock correlation of Kurdistan petroleum. *Org. Geochem.* **2018**, *117*, 22–30. [CrossRef]
12. Gvirtzman, Z.; Said-Ahmad, W.; Ellis, G.; Hill, R.; Moldowan, J.M.; Wei, Z.; Amrani, A. Compound-specific sulfur isotope analysis of thiadiamondoids of oils from the Smackover Formation, USA. *Geochim. Cosmochim. Acta* **2015**, *167*, 144–161. [CrossRef]
13. Zhu, X.; Chen, J.; He, L.; Wang, Y.; Zhang, K. Geochemical characteristics and source correlation of hydrocarbons in the Well Luosi 2 of Maigaiti Slope, Tarim Basin, China. *Nat. Gas Geosci.* **2017**, *28*, 566–574.
14. Liu, Z.; Zhang, F.; Gao, S.; Yue, Y. Ordovician stratigraphic divisions and correlation of Maigaiti slope in Tarim Basin and its significance. *Glob. Geol.* **2016**, *35*, 708–716. (In Chinese with English abstract) [CrossRef]
15. Li, D. Study on Dynamic Adjustment Mechanism of Late Himalayan Oil and Gas Reservoirs in Bashitupu Oilfield, Tarim Basin. Master's Thesis, Guizhou University, Guizhou, China, 2017.
16. Peters, K.; Walters, C.; Moldowan, J. *The Biomarker Guide: Biomarkers and Isotopes in Petroleum Exploration and Earth History*; Cambridge University Press: Cambridge, UK, 2005.
17. Seifert, W.K.; Moldowan, J.M. Use of biological markers in petroleum exploration. *Methods Geochem. Geophys.* **1986**, *24*, 261–290.
18. Asif, M.; Fazeelat, T.; Grice, K. Petroleum geochemistry of the Potwar Basin, Pakistan: 1. Oil–oil correlation using biomarkers, $\delta^{13}C$ and δD. *Org. Geochem.* **2011**, *42*, 1226–1240. [CrossRef]
19. Li, F.; Zhu, G.; Lv, X.; Zhang, Z.; Wu, Z.; Xue, N.; He, T.; Wang, R. The disputes on the source of Paleozoic marine oil and gas and the determination of the Cambrian system as the main source rocks in Tarim Basin. *Acta Pet. Sin.* **2021**, *42*, 1417–1436. (In Chinese with English abstract) [CrossRef]
20. Li, S.; Amrani, A.; Pang, X.; Yang, H.; Said-Ahmad, W.; Zhang, B.; Pang, Q. Origin and quantitative source assessment of deep oils in the Tazhong Uplift, Tarim Basin. *Org. Geochem.* **2015**, *78*, 1–22. [CrossRef]
21. He, T.; Li, W.; Lu, S.; Yang, E.; Jing, T.; Ying, J.; Zhu, P.; Wang, X.; Pan, W.; Chen, Z. Distribution and isotopic signature of 2-alkyl-1,3,4-trimethylbenzenes in the Lower Paleozoic source rocks and oils of Tarim Basin: Implications for the oil-source correlation. *Petrol. Sci.* **2022**, *19*, 2572–2582. [CrossRef]
22. Wang, Q.; Huang, H.; Chen, H.; Zhao, Y. Secondary alteration of ancient Shuntuoguole oil reservoirs, Tarim Basin, NW China. *Mar. Petrol. Geol.* **2020**, *111*, 202–218. [CrossRef]
23. Hanin, S.; Adam, P.; Kowalewski, I.; Huc, A.Y.; Carpentier, B.; Albrecht, P. Bridgehead alkylated 2-thiaadamantanes: Novel markers for sulfurisation occurring under high thermal stress in deep petroleum reservoirs. *Chem. Comm.* **2002**, *33*, 1750–1751. [CrossRef]

24. Wei, Z.B.; Walters, C.C.; Moldowan, J.M.; Mankiewicz, P.J.; Pottorf, R.J.; Xiao, Y.T.; Maze, W.; Nguyen, P.T.H.; Madincea, M.E.; Phan, N.T.; et al. Thiadiamondoids as proxies for the extent of thermochemical sulfate reduction. *Org. Geochem.* **2012**, *44*, 53–70. [CrossRef]
25. Dahl, J.E.; Moldowan, J.M.; Peters, K.E.; Claypool, G.E.; Rooney, M.A.; Michael, G.E.; Mello, M.R.; Kohnen, M.L. Diamondoid hydrocarbons as indicators of natural oil cracking. *Nature* **1999**, *399*, 54–57. [CrossRef]
26. Fang, C.; Xiong, Y.; Liang, Q.; Li, Y. Variation in abundance and distribution of diamondoids during oil cracking. *Org. Geochem.* **2012**, *47*, 1–8. [CrossRef]
27. Radke, M.; Welte, D.H. The methylphenanthrene index (MPI): A maturity parameter based on aromatic hydrocarbons. *Adv. Org. Geochem.* **1983**, *1981*, 504–512.
28. Radke, M.; Welte, D.H.; Willsch, H. Maturity parameters based on aromatic hydrocarbons: Influence of the organic matter type. *Org. Geochem.* **1986**, *10*, 51–63. [CrossRef]
29. Van Graas, G.W. Biomarker maturity parameters for high maturities: Calibration of the working range up to the oil/condensate threshold. *Org. Geochem.* **1990**, *16*, 1025–1032. [CrossRef]
30. Peters, K.E.; Moldowan, J.M. *The Biomarker Guide: Interpreting Molecular Fossils in Petroleum and Ancient Sediments*; Prentice Hall: Englewood Cliffs, NJ, USA, 1993.
31. Li, M.; Wang, T.; Paul, G.L.; Wang, C.; Shi, S. The significance of 24-norcholestanes, triaromatic steroids and dinosteroids in oils and Cambrian–Ordovician source rocks from the cratonic region of the Tarim Basin, NW China. *Appl. Geochem.* **2012**, *27*, 1643–1654. [CrossRef]
32. Chen, Z.; Wang, T.; Li, M.; Yang, F.; Cheng, B. Biomarker geochemistry of crude oils and Lower Paleozoic source rocks in the Tarim Basin, western China: An oil-source rock correlation study. *Mar. Petrol. Geol.* **2018**, *96*, 94–112. [CrossRef]
33. Fan, P.; Philp, P.P.; Li, Z.; Ying, G. Geochemical characteristics of aromatic hydrocarbons of crude oils and source rocks from different sedimentary environments. *Org. Geochem.* **1990**, *16*, 427–435. [CrossRef]
34. He, T.; Lu, S.; Li, W.; Tan, Z.; Zhang, X. Effect of Salinity on Source Rock Formation and Its Control on the Oil Content in Shales in the Hetaoyuan Formation from the Biyang Depression, Nanxiang Basin, Central China. *Energ. Fuel.* **2018**, *32*, 6698–6707. [CrossRef]
35. Didyk, B. Organic geochemical indicators of palaeoenvironmental conditions of sedimentation. *Nature* **1978**, *272*, 216–222. [CrossRef]
36. Evenick, J.C. Evaluating source rock organofacies and paleodepositional environments using bulk rock compositional data and pristane/phytane ratios. *Mar. Pet. Geol.* **2016**, *78*, 507–515. [CrossRef]
37. Hughes, W.B.; Holba, A.G.; Dzou, L.I.P. The ratios of dibenzothiophene to phenanthrene and pristane to phytane as indicators of depositional environment and lithology of petroleum source rocks. *Geochem. Cosmochim. Acta* **1995**, *59*, 3581–3598. [CrossRef]
38. Schwark, L.; Empt, P. Sterane biomarkers as indicators of palaeozoic algal evolution and extinction events. *Palaeogeogr. Palaeoclimatol. Palaeoecol.* **2006**, *240*, 225–236. [CrossRef]
39. Kelly, A.E.; Love, G.D.; Zumberge, J.E.; Summons, R.E. Hydrocarbon biomarkers of Neoproterozoic to lower Cambrian oils from eastern siberia. *Org. Geochem.* **2011**, *42*, 640–654. [CrossRef]
40. Bhattacharya, S.; Dutta, S.; Summons, R.E. A distinctive biomarker assemblage in an InfraCambrian oil and source rock from western India: Molecular signatures of eukaryotic sterols and prokaryotic carotenoids. *Precambrian Res.* **2016**, *290*, 101–112. [CrossRef]
41. Thode, H.G. Sulfur isotope ratios in petroleum research and exploration: Williston Basin. *AAPG Bull.* **1981**, *65*, 1527–1535. [CrossRef]
42. Orr, W.L. Kerogen/asphaltene/sulphur relationships in sulphur-rich Monterey oils. *Org. Geochem.* **1986**, *10*, 499–516. [CrossRef]
43. Liu, J.; Tian, L.; Cui, H.; Chen, Y.; Zhang, N. Genesis Analyses of Oil, Gas, Water and Its Significance for Exploration in the Oil-gas Field of Bachu-Maigaiti Slope Area, Tarim Basin. *Mar. Orig. Pet. Geol.* **2017**, *22*, 62–68. (In Chinese with English abstract) [CrossRef]
44. Amrani, A.; Lewan, M.D.; Aizenshtat, Z. Stable sulfur isotope partitioning during simulated petroleum formation as determined by hydrous pyrolysis of Ghareb Limestone, Israel. *Geochim. Cosmochim. Acta* **2005**, *69*, 5317–5331. [CrossRef]
45. He, T.; Li, W.; Lu, S.; Yang, E.; Jing, T.; Ying, J.; Zhu, P.; Wang, X.; Pan, W.; Zhang, B.; et al. Quantitatively unmixing method for complex mixed oil based on its fractions carbon isotopes: A case from the Tarim Basin, NW China. *Petrol. Sci.* **2023**, *20*, 102–113. [CrossRef]